BRAIN
ORIGINAL ARTICLE

Changes in the language system as amyloid-β accumulates

Mariska Reinartz,[1,†] Silvy Gabel,[1,†] Jolien Schaeverbeke,[1] Karen Meersmans,[1] Katarzyna Adamczuk,[2] Emma Susanne Luckett,[1] Steffi De Meyer,[1] Koen Van Laere,[3,4] Stefan Sunaert,[5] Patrick Dupont[1] and Rik Vandenberghe[1,6,7]

[†]These authors contributed equally to this work.

Language dysfunction is common in Alzheimer's disease. There is increasing interest in the preclinical or asymptomatic phase of Alzheimer's disease.

Here we examined in 35 cognitively intact older adults (age range 52–78 years at baseline, 17 male) in a longitudinal study design the association between accumulation of amyloid over a 5–6-year period, measured using PET, and functional changes in the language network measured over the same time period using task-related functional MRI. In the same participants, we also determined the association between the longitudinal functional MRI changes and a cross-sectional measure of tau load as measured with ^{18}F-AV1451 PET.

As predicted, the principal change occurred in posterior temporal cortex. In the cortex surrounding the right superior temporal sulcus, the response amplitude during the associative-semantic versus visuo-perceptual task increased over time as amyloid load accumulated ($P_{corrected}$ = 0.008). In a whole-brain voxel-wise analysis, amyloid accumulation was also associated with a decrease in response amplitude in the left inferior frontal sulcus ($P_{corrected}$ = 0.009) and the right dorsomedial prefrontal cortex ($P_{corrected}$ = 0.005). In cognitively intact older adults, cross-sectional tau load was not associated with longitudinal changes in functional MRI response amplitude.

Our findings confirm the central role of the neocortex surrounding the posterior superior temporal sulcus as the area of predilection within the language network in the earliest stages of Alzheimer's disease. Amyloid accumulation has an impact on cognitive brain circuitry in the asymptomatic phase of Alzheimer's disease.

1 Laboratory for Cognitive Neurology, Department of Neurosciences, Leuven Brain Institute, KU Leuven, 3000 Leuven, Belgium
2 Bioclinica LAB, Newark, CA 94560, USA
3 Division of Nuclear Medicine, UZ Leuven, 3000 Leuven, Belgium
4 Nuclear Medicine and Molecular Imaging, Department of Imaging and Pathology, KU Leuven, 3000 Leuven, Belgium
5 Translational MRI, KU Leuven, 3000 Leuven, Belgium
6 Alzheimer Research Centre KU Leuven, Leuven Brain Institute, 3000 Leuven, Belgium
7 Neurology Department, University Hospitals Leuven, 3000 Leuven, Belgium

Correspondence to: Rik Vandenberghe
Neurology Department, University Hospitals Leuven
Herestraat 49, 3000 Leuven, Belgium
E-mail: rik.vandenberghe@uz.kuleuven.ac.be

Received April 23, 2021. Revised July 08, 2021. Accepted August 12, 2021. Advance access publication September 17, 2021

Keywords: longitudinal study; fMRI; amyloid PET; 18F-AV1451; Alzheimer's disease

Abbreviations: BOLD = blood oxygen-level dependent; IFS = inferior frontal sulcus; MMSE = Mini-Mental State Examination; MTG = middle temporal gyrus; STS = superior temporal sulcus; SUVR = standardized uptake value ratio; VOI = volume of interest

Introduction

Language dysfunction is common in the early stage of typical Alzheimer's disease.[1–3] There is an increasing interest in the asymptomatic phase of Alzheimer's disease, where Alzheimer's disease-related brain pathology is present but symptoms are not yet clinically apparent.[4,5] A critical intermediary level between molecular aggregates and clinical manifestations consists of the way in which cognitive brain systems are able to adapt to amyloid-β-related pathology. This intermediary level is only accessible by means of *in vivo* techniques of measuring brain function, such as functional MRI. Functional changes in cognitive brain circuits during the asymptomatic phase of Alzheimer disease are still poorly understood.

Previous studies of changes in cognitive brain circuits in asymptomatic Alzheimer's disease have mainly focused on the episodic memory system.[6–9] These studies have led to a biphasic model of hippocampal activity in Alzheimer's disease where a compensatory increase in the preclinical and mild cognitive impairment stage is followed by hypo-activation in the Alzheimer's disease dementia stage.[10] Alternatively, the excess hippocampal activity in amnestic mild cognitive impairment may also be harmful as drug-induced reduction of hippocampal hyperactivity has led to improved episodic memory performance.[11,12]

Even if the amnestic phenotype is the most defining characteristic of Alzheimer's disease, language changes are highly prevalent in typical Alzheimer's disease, even in an early stage.[1–3,13] Studying the functional neuroanatomy of language and semantic processing requires a task paradigm suitable for functional MRI that reliably activates the widely distributed language and associative-semantic network with low between-subject and high within-subject consistency. Such task-related functional MRI studies have highlighted the vulnerability of the posterior third of the superior temporal sulcus (STS) and of the middle temporal gyrus (MTG) in the asymptomatic,[4,14] mild cognitive impairment[15,16] and early dementia stages of Alzheimer's disease.[17] In the early dementia phase of amyloid biomarker-positive Alzheimer's disease, the left posterior STS and the posterior MTG are decreased in activity during associative-semantic versus visuo-perceptual processing. By contrast, the homologous right-sided region showed an increase in activity and this correlated positively with offline Boston Naming Test scores, suggestive of a compensatory mechanism.[17] Seed-based resting-state functional connectivity between the left posterior MTG and the homologous contralateral node is also decreased in Alzheimer's disease dementia.[18] In cognitively normal older adults, the only region where activity during associative-semantic versus visuo-perceptual processing correlates with amyloid load in a whole-brain analysis is the posterior third of the left STS[14]: response amplitude in the left STS was higher with higher amyloid load. Higher amyloid load also correlated with longer reaction times during an offline confrontation naming task.[14] This series of task-related and resting-state functional MRI studies in different phases of Alzheimer's disease demonstrates the vulnerability of the posterior STS and MTG as nodes of the language network to amyloid-β-related pathology.[14,15,17,18] The findings could be compatible with a biphasic model where the left posterior temporal cortex first shows increased activity with a higher amyloid load and subsequently fails to activate. In this model, the right posterior temporal cortex may show a compensatory increase in activity in order to maintain adequate performance. Longitudinal studies, however, are needed to test this hypothesis further.

Here we tested longitudinally over a 5–6-year interval how activity in the language network changes in cognitively intact older adults in relation to changes in amyloid load. Based on the cited evidence, we hypothesized that an increase in amyloid-β would be associated with changes in activity in left or right posterior STS/MTG. Since it is commonly accepted that functional brain changes may relate more to deposition of tau aggregates than to amyloid-β,[19,20] we also examined the relationship with tau aggregates measured cross-sectionally using ^{18}F-AV1451.

Materials and methods

Study participants

Thirty-five cognitively intact healthy older adults participated in the current study. All belonged to the Flemish-Prevent AD Cohort KU Leuven (F-PACK), a larger longitudinal community-recruited study cohort of 180 cognitively intact older individuals.[21] The F-PACK cohort was recruited in three waves of 60 participants each. The first wave was recruited between 2009 and 2012 and received ^{18}F-flutemetamol PET as well as task-related functional MRI of the language system at baseline. All participants of the first wave of the F-PACK study cohort were invited to participate in the current amyloid and tau PET plus task-related functional MRI study between 2015 and 2019. Twenty-four participants of the first wave declined participation in the current study. There was no significant difference in baseline characteristics between subjects who consented to participate in the current study and those who refused (Table 1), according to unpaired two-tailed *t*-tests and Mann-Whitney U-tests depending on normality. Of the 35 participants, one had to be excluded subsequently based on excessive head movement during the functional MRI scan (see 'Image analysis' section). For a detailed description of the full F-PACK inclusion criteria, refer to the Supplementary material and also previous reports.[21]

The local Ethics Committee for Clinical Studies UZ/KU Leuven approved the study. Written informed consent was obtained from all participants in accordance with the Declaration of Helsinki.

Standard neuropsychological assessment

All participants underwent baseline and follow-up testing for general cognition [Clinical Dementia Rating (CDR) and Mini Mental State Examination (MMSE)], episodic memory [Auditory Verbal Learning Test (AVLT) and Buschke Selective Reminding Test (BSRT)], language, fluid intelligence/reasoning and executive functioning. Language and semantic processing were assessed using the Boston Naming Test.[22] Fluency was assessed using a 1-min Animal Verbal Fluency task and a Letter Verbal Fluency task. The Dutch version of the Psycholinguistic Assessment of Language Processing in Aphasia (PALPA) subtest 49 was used to probe verbal associative-semantic processing.[23] Executive functioning was measured with Trail Making Test (TMT) A and B. Fluid intelligence/

Table 1 Sample characteristics at baseline of the participants of the current study and the refusers

	Participants	Refusers	Statistics
Centiloid value	8.9 [–8.3 to 44.7]	6.8 [–14.1 to 69.5]	$U = 567$, $P = 0.08$
MMSE (/30)	29.1 [27.0 to 30.0]	28.8 [27.0 to 30.0]	$U = 528.5$, $P = 0.21$
AVLT total learning (/75)	51.6 [33.0 to 65.0]	47.0 [27.0 to 67.0]	$T = 1.95$, $P = 0.06$
AVLT % delayed recall	89.7 [57.1 to 116.7]	87.5 [42.9 to 150.0]	$U = 494$, $P = 0.51$
Buschke mean total retention (/12)	8.9 [7.1 to 10.3]	8.8 [4.8 to 10.5]	$U = 344.5$, $P = 0.12$
Buschke delayed recall (/12)	9.6 [5.0 to 12.0]	9.1 [3.0 to 12.0]	$U = 517$, $P = 0.32$
BNT (/60)	54.0 [41.0 to 60.0]	51.8 [38.0 to 60.0]	$U = 546.5$, $P = 0.15$
AVF (# words)	21.3 [14.0 to 32.0]	19.4 [9.0 to 34.0]	$T = 1.49$, $P = 0.14$
LVF (# words)	34.3 [14.0 to 59.0]	32.6 [16.0 to 51.0]	$T = 0.65$, $P = 0.52$
PALPA49 (/30)	26.6 [23.0 to 29.0]	27.1 [21.0 to 30.0]	$U = 369$, $P = 0.23$
RPM (/60)	43.8 [17.0 to 55.0]	36.9 [5.0 to 58.0]	$U = 571$, $P = 0.07$
TMT B/A	2.5 [1.2 to 5.3]	2.7 [0.9 to 5.5]	$U = 398$, $P = 0.45$

Values are presented as mean [range]. Statistics represent *t*-test and Mann-Whitney U-test depending on normality of the data. AVF = Animal Verbal Fluency; AVLT = Auditory Verbal Learning Test; BNT = Boston Naming Test; LVF = Letter Verbal Fluency; PALPA49 = Psycholinguistic Assessment of Language Processing in Aphasia subtest 49; RPM = Standard Raven's Progressive Matrices; TMT B/A = Trail Making Test ratio B/A.

reasoning was assessed using the 60 items of the Standard Raven's Progressive Matrices (RPM).

Table 2 shows demographic characteristics and average standard deviation (SD) cognitive test scores for the total sample of cognitively intact older adults ($n = 35$). The same tests were administered every 2 years for a total follow-up period of 10 years. The average follow-up interval for this study was 75.6 (SD 17.7) months.

Experimental language tests

Given our *a priori* hypothesis of early involvement of left posterior STS and given its possible role in lexical-semantic retrieval,[15] the experimental language tests conducted outside the functional MRI scanner consisted of a computerized version of confrontation naming and of lexical decision.[14] The details of these tests have been described before[14] and are also provided in the Supplementary material. In summary, for confrontation naming, a computerized version of the picture naming task from Laiacona and Capitani[24] was used.[25] Voice recordings were manually analysed in the Audacity Cross-Platform Sound Editor version 2.4.2 (https://www.audacityteam.org/; accessed 30 September 2021). Reaction times were measured for the correct responses from the onset of the stimulus to the onset of the naming response. Accuracy was measured as percentage correct responses.

For lexical decision, a computerized version of the visual lexical decision test from the Dutch version of the PALPA (item 24)[23] was administered, as described before.[14] Reaction times were measured for correct responses from the onset of the stimulus to the time of the button press. A' was used as our non-parametric accuracy measure, as the data were not normally distributed, as assessed with the Shapiro-Wilk test.[26,27] In addition, we determined the index of response bias (Table 2).[27]

Image acquisition

Functional and structural MRI data were acquired at two time points, one at baseline (2009–12, hereafter referred to as time point 1) and one at follow-up (2015–19, hereafter referred to as time point 2) with a mean interval of 69 months (SD: 13.2, range: 52–106 months). The same scanning sequence was used for the two time points.

At time point 1, 21 subjects were scanned on a 3 T Philips Achieva system equipped with a 32-channel receive-only head coil (Philips SENSitivity Encoding head coil). Fifteen other subjects were scanned on a 3 T Philips Intera system equipped with an 8-channel receive-only head coil (Philips SENSitivity Encoding head coil), which was in use prior to the installation of the 3 T Philips Achieva. At time point 2 all subjects were scanned on the 3 T Philips Achieva system equipped with a 32-channel receive-only head coil (Philips SENSitivity Encoding head coil). There were no statistically significant differences of sex ($P = 0.79$) (chi-square test), age ($P = 0.49$), MMSE ($P = 0.92$), baseline amyloid ($P = 0.59$) or amyloid accumulation ($P = 0.29$) (Kolmogorov-Smirnov comparison of two datasets) between subjects scanned on the Intera versus the Achieva system. Scanner type was included as a covariate of no interest for all analyses.

Sequence parameters were the same for both scanners: a high-resolution T_1-weighted structural scan was obtained using a 3D turbo field echo sequence (coronal inversion recovery prepared 3D gradient-echo images, inversion time 900 ms, repetition time = 9.6 ms, echo time = 4.6 ms, flip angle 8°, field of view = 250 × 250 mm, 182 slices; voxel size 0.98 × 0.98 × 1.2 mm^3). Functional MRIs were acquired using T_2^* echo-planar images (50 transverse slices, voxel size 2.5 × 2.5 × 2.5 mm^3; repetition time = 3000 ms, echo time = 30 ms, flip angle 90°, field of view 200 × 200 mm).

Functional MRI

Stimuli and tasks

Stimuli were projected onto a high-resolution screen (1024 × 768 pixels, refresh rate 60 Hz) using Presentation 14.8 (NeuroBehavioural Systems, Albany, CA, USA). The functional MRI paradigm has been described in detail before.[15,17,28–32] In summary, the experimental design was factorial.[28] The first factor 'task' had two levels: associative-semantic (Fig. 1, blue and purple) versus visuo-perceptual judgement (Fig. 1, cyan and yellow). The second factor 'input modality' also had two levels: printed words (Fig. 1, blue and cyan) versus pictures (Fig. 1, purple and yellow). The associative-semantic condition was derived from the Pyramids and Palm Trees Test,[33] a classical neuropsychological test of associative-semantic processing for words and pictures. During a trial, a triplet of stimuli was presented for 5250 ms, one stimulus on top (the sample stimulus) and one in each lower quadrant (the test stimuli), at 4.6° eccentricity (mean picture size was 3.7° and mean letter size 1.2°), followed by a 1500 ms interstimulus interval. Subjects were asked to press a left- or right-hand key depending on which of the two test stimuli matched the sample stimulus more closely in meaning. A given triplet was presented in either the picture or the word format and this was counterbalanced across subjects. In the visuo-perceptual control condition, a picture or word stimulus was presented in three different sizes (mean picture size was 3.7° and mean letter size 1.2°). Subjects had

Table 2 Demographic characteristics and cognitive test scores at baseline and follow-up

Sex, male/female (% male)	17/18 (48.6%)	
Education, years,	12.7 (2.7) [6.0 to 19.0]	
APOE ε4 carriers, *n* (%)	19 (54.3%)	
BDNF *met* carriers, *n* (%)	14 (40%)	
	Baseline	**Follow-up**
Age, years	65.4 (6.1) [52.0 to 78.0]	71.6 (5.7) [59.0 to 83.0]
Centiloids	8.4 (11.2) [–8.3 to 44.7]	21.6 (27.3) [–6.6 to 89.5]
CDR 0.5, *n*	0	2
MMSE (/30)	29.1 (0.8) [27.0 to 30.0]	29.3 (0.9) [26.0 to 30.0]
AVLT total learning (/75)	51.5 (9.0) [30.0 to 65.0]	51.6 (10.8) [27.0 to 73.0]
AVLT delayed recall, %	89.7 (12) [57.1 to 116.7]	86.9 (14.4) [50.0 to 107.1]
Buschke mean score (/12)	8.8 (0.9) [7.1 to 10.5]	8.0 (1.9) [2.4 to 11.5]
Buschke delayed recall (/12)	9.5 (1.9) [5.0 to 12.0]	7.9 (3.2) [0.0 to 12.0]
BNT (/60)	53.8 (3.9) [41.0 to 60.0]	55.9 (2.8) [49.0 to 60.0]
LVF (# words)	35.1 (9.5) [14.0 to 59.0]	30.2 (11.3) [11.0 to 49.0]
AVF (# words)	21.1 (4.8) [14.0 to 32.0]	23.3 (8.7) [14.0 to 50.0]
PALPA49 (/30)	26.6 (1.6) [23.0 to 29.0]	27.3 (1.5) [23.0 to 30.0]
RPM (/60)	43.6 (7.5) [17.0 to 55.0]	40.6 (7.5) [23.0 to 54.0]
TMT B/A	2.5 (0.9) [1.2 to 5.3]	2.8 (1.1) [1.5 to 5.5]
Confrontation naming RT, ms[a]	1946.4 (249.4) [1506.8 to 2578.3]	1758.6 (266.2) [1415.6 to 2449.7]
Confrontation naming accuracy, %[a]	92.2 (4.1) [81.7 to 98.3]	91.3 (5.1) [78.3 to 98.3]
Lexical decision RT, ms	1088.0 (224.3) [790.6 to 1855.4]	1067.4 (205.4) [768.0 to 1630.1]
Lexical decision accuracy (A')	0.98 (0.02) [0.91 to 1.00]	0.98 (0.01) [0.92 to 1.00]
Lexical decision index of bias (B''_D)	0.23 (0.44) [–0.77 to 0.89]	0.05 (0.44) [–0.88 to 0.88]

Values are presented as mean (SD) [range]. AVF = Animal Verbal Fluency; AVLT = Auditory Verbal Learning Test; BNT = Boston Naming Test; CDR = Clinical Dementia Rating; LVF = Letter Verbal Fluency; PALPA49 = Psycholinguistic Assessment of Language Processing in Aphasia subtest 49; RPM = Standard Raven's Progressive Matrices; RT = reaction time; TMT B/A = Trail Making Test ratio B/A.

[a]Confrontation naming reaction times and accuracies are based on *n* = 28 participants, due to missing data of seven participants.

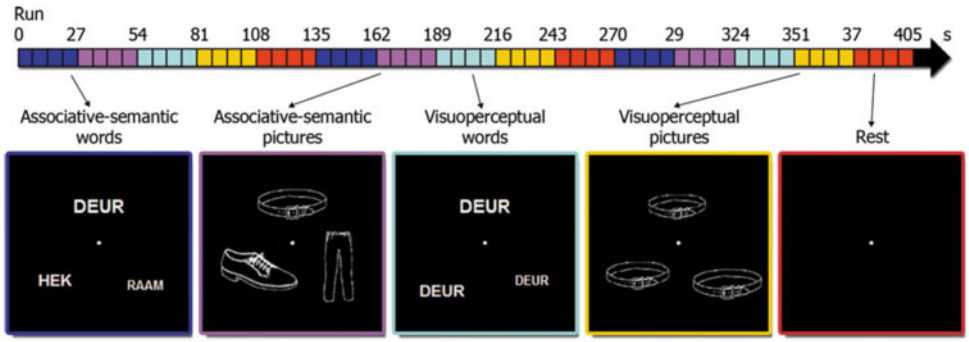

Figure 1 Experimental paradigm. The horizontal arrow at the *top* of the figure shows a timeline of one functional MRI run, with each condition (i.e. associative-semantic words/pictures and visuo-perceptual words/pictures as well as a rest condition) indicated in its respective colour. The order of conditions was randomized for each run and subject. Translation from Dutch to English: *deur* = door, *hek* = fence, *raam* = window.

to press a left- or right-hand key depending on which of the two test stimuli matched the sample stimulus more closely in size on the screen. An epoch, i.e. a block of trials belonging to the same condition, consisted of four trials (total duration 27 s). The fifth condition consisted of a resting baseline condition during which a fixation point was presented in the centre of the screen (Fig. 1, red). During each functional MRI run (five runs in total), a series of the five epoch types was replicated three times (Fig. 1, timeline). The order of conditions was pseudorandom and differed across runs of the same subject.

Subjects received a practice session before entering the scanner. In this session, we determined which size difference (9%, 6%, 3% or 1%) for the visuo-perceptual conditions was needed for each individual subject to obtain comparable accuracies as for the associative-semantic conditions so as to match overall task difficulty. This size difference was then used for the visuo-perceptual condition during functional MRI.

Image analysis

All analyses were performed using Statistical Parametric Mapping 12 [SPM12 software (Wellcome Trust Centre for Neuroimaging, London, UK, http://www.fil.ion.ucl.ac.uk/spm; accessed 30 September 2021)] running on MATLAB 2014b (MathWorks, Natick, MA, USA). The procedure for longitudinal functional MRI analysis was inspired by the longitudinal voxel-based brain morphometry pipeline described by Chételat *et al.*[34] and is described in detail in the Supplementary material and Supplementary Fig. 1. In summary, functional MRI scans of each subject were realigned for time point 1 and for time point 2 separately, and co-registered with

their respective corresponding structural MRI. The structural MRI scans from the two time points were co-registered and normalized and the same normalization matrix was applied to the functional MRI scans. Normalized functional MRI images were smoothed using a $8 \times 8 \times 8$ mm^3 Gaussian kernel. One subject was excluded due to excessive head movement (rotation $>3°$ and translation >3 mm).

Flutemetamol PET

Image acquisition

^{18}F-flutemetamol was obtained from Nucleis, and was produced under GMP conditions. As described before,[35–38] images were acquired on a 16-slice Siemens Biograph PET/CT scanner (Siemens). The ^{18}F-flutemetamol PET tracer was injected intravenously as a bolus (mean activity: 151.2 MBq, SD: 8.3, range: 137.9–192.5 MBq) in an antecubital vein. Image acquisition began 90 min after tracer injection and lasted for 30 min. Prior to the PET scan, a low-dose CT scan of the head (11 mA) was performed for attenuation correction. Random and scatter corrections were also applied. Images were reconstructed using ordered subsets expectation maximization (OSEM; four iterations $\times$ 16 subsets).

Image analysis

The details of the procedure for ^{18}F-flutemetamol PET analysis have been described before[14,21,39] and are also described in the Supplementary material. Using a standard procedure, an ^{18}F-flutemetamol standardized uptake value ratio (SUVR) in a composite cortical volume of interest (VOI) was derived from the ^{18}F-flutemetamol scans. No partial volume correction was applied as this may introduce additional noise in amyloid PET data in cognitively intact older adults.[40]

PIB imaging

The follow-up amyloid scan was performed by means of ^{11}C-Pittsburgh Compound B (PIB) due to unavailability of the ^{18}F-flutemetamol tracer in Belgium for research at the time of follow-up. ^{11}C-PIB was produced locally under GMP license. ^{11}C-PIB PET was acquired dynamically over a period of 60 min on a 16-slice Biograph PET/CT scanner (Siemens). For the details of acquisition and analysis, refer to the Supplementary material. Using a standard procedure, global and regional ^{11}C-PIB SUVRs were calculated between 40 and 60 min post-injection using SPM12. The mean ^{11}C-PIB SUVR measure was calculated in the same composite cortical VOI as for the ^{18}F-flutemetamol images. No partial volume correction was applied.[40]

Measure of longitudinal change in amyloid load

For the primary outcome analysis, we used a continuous measure of longitudinal change in amyloid load in the composite cortical VOI. To analyse amyloid load using two different tracers, corresponding SUVR values were first transformed to the Centiloid (CL) scale, which was used for both the first and the second scan. The difference in Centiloid values between the two time points was used as outcome measure. To this end, the in-house processing procedures to obtain ^{18}F-flutemetamol and ^{11}C-PIB $SUVR_{comp}$ values were first calibrated against the standard Centiloid method,[41] using an independent dataset as described before for ^{18}F-flutemetamol[39] and an independent in-house dataset of cognitively intact older controls for ^{11}C-PIB.[42] This yielded the following conversion formulae for ^{18}F-flutemetamol[39] (Equation 1) and ^{11}C-PIB (Equation 2).

$$CL_{flutemetamol} = 127.6 \times SUVR_{90-110} - 149 \quad (1)$$

$$CL_{PIB} = 132.53 \times SUVR_{40-60} - 147.64 \quad (2)$$

These formulae were then applied to the ^{18}F-flutemetamol SUVR and ^{11}C-PIB SUVR data from the 35 participants in the current study, respectively.

To determine amyloid-positivity in this cohort, we classified cases in a binary way based on a pathologically validated Centiloid cut-off of 23.5.[43] We also applied a separate classification based on three levels: low ($CL < 10$), intermediate ($CL > 10$) and high ($CL > 50$) amyloid load.[44] This is purely for descriptive reasons since the primary and secondary analyses all make use of amyloid load as a continuous variable.

Tau PET imaging

Participants received a dynamic ^{18}F-AV1451 PET scan on a 16-slice Biograph PET/CT scanner (Siemens). The procedures for tau PET acquisition and analysis were standard and are described in detail in the Supplementary material. In summary, we calculated distributed volume ratio (DVR) images and derived tau PET load in an early metaVOI. The DVR in this early metaVOI was used for further analysis. We also used the tau PET to determine which cases were positive for tau in the early metaVOI with the cut-off set at SUVR $\geqslant$ 1.38. To determine tau-positivity, we made use of SUVRs since our independent reference group on which the positivity threshold was based only had static acquisition (Supplementary material).

Statistical analyses

Voxel-wise statistical analyses were conducted in SPM12 software running on MATLAB 2014b. All standard statistical analyses were conducted with R statistical software version 4.0.3 (The R Foundation for Statistical Computing; https://cran.r-project.org; accessed 30 September 2021). *P*-values were considered significant when meeting a two-tailed α threshold of 0.05. Correction for multiple comparisons was performed using Bonferroni correction. Outliers were assessed using the Grubb's test (https://www.graphpad.com/quickcalcs/grubbs2/; accessed 30 September 2021). In case of missing data, only the available data were used in the analyses.

Prior to statistical analyses, the Shapiro-Wilk test was used to check for normality of the data. In case the distribution of a variable differed significantly from normality ($\alpha < 0.05$), non-parametric statistics were used for this variable.

The neuropsychological test scores were entered into a latent growth curve analysis using the R package *lavaan*[45] (http://www.jstatsoft.org/v48/i02/; accessed 30 September 2021) to determine whether performance on offline standard cognitive tasks changed over time at the group level.[21] To evaluate whether amyloid accumulation was associated with neuropsychological changes, a linear regression analysis was also carried out with amyloid accumulation as regressor and the slope of a selection of the main conventional neuropsychological test scores (BSRT total retention,[21] Animal Verbal Fluency, Boston Naming Test, Letter Verbal Fluency, Standard Raven's Progressive Matrices and Trail Making Test B/A ratio) as outcome variable.

The Kolmogorov-Smirnov test for comparison of two datasets was used to compare change in functional MRI response between subjects scanned on the Intera versus the Achieva system at baseline.

Reaction times and accuracies of the behavioural task during functional MRI were calculated per condition [associative-semantic task with words (Sem W) and with pictures (Sem P), and visuo-perceptual task with words (Visuo W) and with pictures (Visuo P);

Table 3 Performance during functional MRI experiments at baseline and follow-up

	Baseline		Follow-up		Statistics	
	RT, ms	Accuracy, % correct	RT, ms	Accuracy, % correct	RT	Accuracy
Sem W	2644 (476)	88.7 (7.6)	3190 (416)	85.4 (8.2)	$T = -7.34$	$T = 1.93$
					$P < 0.0001$	$P = 0.06$
Sem P	2817 (543)	81.2 (9.3)	3344 (473)	79.7 (12.8)	$T = -6.59$	$T = 0.595$
					$P < 0.0001$	$P = 0.56$
Visuo W	2448 (438)	79.5 (13.9)	3073 (487)	78.8 (11.9)	$T = -7.12$	$T = 0.21$
					$P < 0.0001$	$P = 0.84$
Visuo P	2656 (495)	80.7 (15.2)	3247 (509)	80.5 (12.1)	$T = -5.88$	$T = 0.045$
					$P < 0.0001$	$P = 0.94$

Values are presented as mean (SD). Statistics represent Bonferroni-corrected *P*-values for pairwise *t*-test as *post hoc* analysis after repeated measures ANOVA. Note that the results are based on $n = 33$ participants, due to missing data of two participants. Statistically significant results are highlighted in bold. RT = reaction time; Sem P/W = associative-semantic task with pictures/words; Visuo P/W = visuo-perceptual task with pictures/words.

Table 3]. A two-way repeated measures ANOVA was performed, using the R package *afex* (https://github.com/singmann/afex; accessed 30 September 2021),[46] to evaluate the effect of the different conditions over time on reaction times and accuracy. The effect of time on both reaction time and accuracy was analysed for every condition using pairwise comparisons *post hoc*. *P*-values were adjusted using the Bonferroni multiple testing correction method.

Primary outcome analysis

Based on prior experiments,[14–17] we predicted that left and right posterior STS and MTG would show decreases or increases in relation to the degree of amyloid accumulation. All analyses were voxel-wise analyses. Two primary voxel-wise outcome analyses were performed, one within a VOI, the other across the whole brain. The VOI was derived from three prior studies using the same paradigm at different Alzheimer's disease stages.[14,15,17] The VOI consisted of the sum of the Brainnetome atlas areas[47] that encompassed the activity foci that showed significant between-group differences during the associative-semantic versus the visuo-perceptual condition in the Alzheimer's disease group versus the controls in these studies.[14,15,17] These Brainnetome atlas areas (labels 81, 82, 121–124) corresponded to the neocortex surrounding the posterior third of the STS bilaterally. These were combined into one single bilateral VOI, which was used for small volume correction (Fig. 4A).

The main analysis consisted of a linear regression analysis where longitudinal change in amyloid load was the predictor variable and longitudinal change in functional MRI response during the associative-semantic minus the visuo-perceptual condition in the VOI was the outcome variable. The longitudinal change in functional MRI response was calculated as the interaction between task (associative-semantic versus visuo-perceptual) and time (baseline versus follow-up). The significance threshold for the VOI-based voxel-wise analyses was set at voxel-level family-wise error (FWE)-corrected $P < 0.05$.

As a second primary analysis, the same analysis was performed using a whole-brain voxel-wise approach, with change in the amyloid load in the composite VOI as predictor, and as outcome variable the change in the blood oxygen level-dependent (BOLD) response during the associative-semantic versus the visuo-perceptual task over time. This whole-brain voxel-wise analysis was thresholded at a significance threshold of whole-brain FWE-corrected cluster-level $P < 0.05$ with the voxel-level set at $P_{uncorrected} < 0.001$.

When we observed significant effects, we also examined how the change in amyloid and the change in functional MRI BOLD response related to changes in the offline behavioural measures using Pearson or Spearman correlations, depending on normality. The normalized change in reaction time and accuracy between time point 2 (t2) versus time point 1 (t1) were calculated for every subject. Normalized values were calculated as: $(t2 - t1) / [(t1 + t2) / 2]$.

When a significant effect was obtained for the analyses of the contrast between the associative-semantic and the visuo-perceptual condition, we examined whether this was present both for the word and the picture condition. We also examined interactions between task and modality.

Secondary outcome analyses

As a secondary analysis, we examined the relationship between the tau load as measured cross-sectionally with ^{18}F-AV1451 PET at the second time point, and the change in BOLD response between the associative-semantic and the visuo-perceptual task between the two time points, both in a region-based and a whole-brain voxel-wise analysis. Tau load was measured based on the early metaVOI.

We also determined whether the study outcome was affected by grey matter volume loss over time. As an atrophy measure, we calculated the percental grey matter volume change between the two time points in MATLAB as $100 \times (GM1 - GM2) / GM1$ in which GM1 and GM2 are the grey matter volumes at time points 1 and 2, respectively. These grey matter volumes were derived from the grey matter maps in Montreal Neurological Institute (MNI) space as the summed value within the posterior temporal VOI or within the whole brain, respectively. For the VOI-based analysis of task-related functional MRI, the grey matter change in the bilateral posterior temporal VOI was calculated and included as covariate in the VOI-based voxel-wise regression analysis between amyloid change and change in functional MRI activity levels. For the whole-brain voxel-wise analysis, the percentual grey matter volume change was calculated for the whole brain and was used as covariate in the whole-brain voxel-wise analyses between amyloid change and change in functional MRI activity levels. As a further analysis, we examined whether grey matter volume change was associated with changes in functional MRI activity level in the posterior temporal VOI or at the whole-brain level. To this end, a voxel-wise linear regression analysis was carried out between the grey matter volume change in the posterior temporal volume and the functional MRI activity change in this VOI (statistical threshold of small-volume corrected $P < 0.05$). We also performed a whole-brain linear regression analysis with global grey matter volume

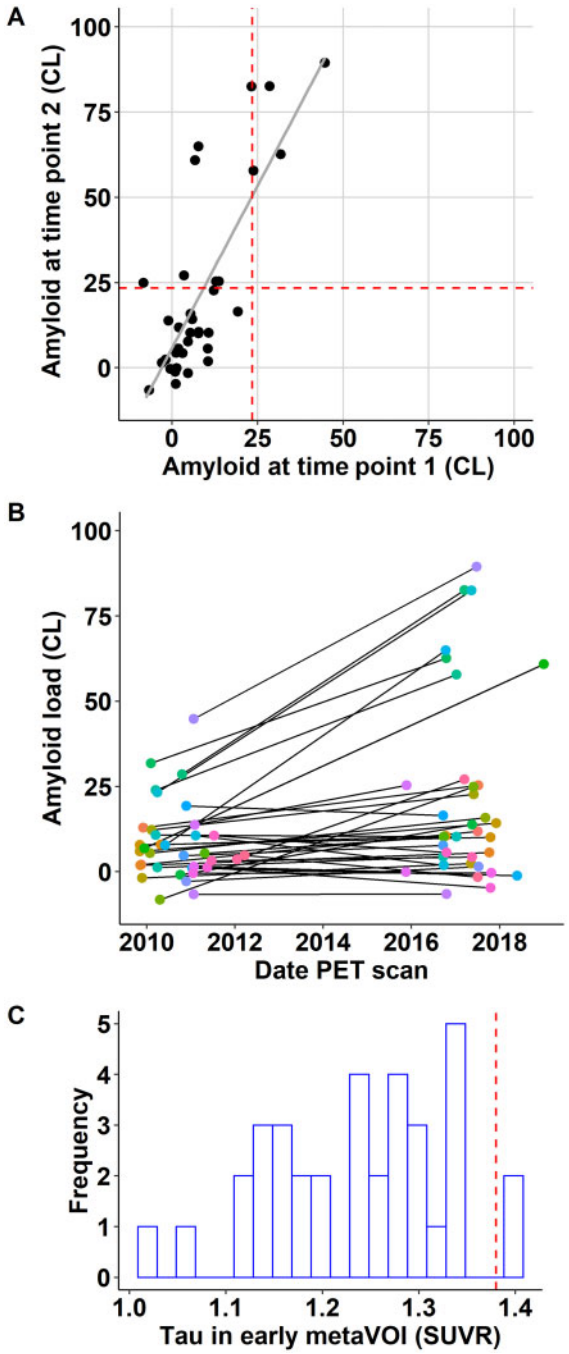

Figure 2 Amyloid accumulation and tau distribution in the current cohort. (**A**) Regression plot between amyloid at time point 1 and time point 2 expressed as Centiloids (CL). The vertical and horizontal dashed red lines indicate the cut-off for amyloid-positivity (CL $\geqslant$ 23.5). (**B**) Amyloid accumulation expressed in Centiloids: amyloid load is shown at the baseline PET date and at the follow-up PET date, corresponding data-points are connected per subject. (**C**) Distribution of tau SUVR values in the early metaVOI, with a bin width of 0.02. The vertical dashed red line indicates the cut-off for tau positivity (SUVR $\geqslant$ 1.38).

change as an independent variable (statistical threshold whole-brain FWE-corrected $P < 0.05$).

Data availability

The data that support the findings of this study are available from the corresponding author upon reasonable request.

Results

In the current cohort, 12 participants (34%) had intermediate amyloid burden (Centiloid range 10–45) and none had high amyloid burden at time point 1, while at time point 2 14 participants (40%) had intermediate (Centiloid range 10–27) and seven participants (20%) had high amyloid burden (Centiloid range 58–89) (Fig. 2A and B). Two participants (5.7%) were tau-positive in the early metaVOI (Fig. 2C).

In two participants the CDR had progressed from a global score of 0 to a global score of 0.5 with corresponding MMSE changes from 30 to 26 (baseline Centiloid: 1.2; change in Centiloid: –5.9) and to 29 of 30 (baseline Centiloid: 5.9; change in Centiloid: 8.2). Group-level neuropsychological performance did not change between baseline and follow-up as assessed with latent growth curve analysis. Neither did the change in scores on the conventional neuropsychological tests correlate with amyloid accumulation.

Statistical analysis of behavioural performance during functional MRI

Based on the prior training session, the size difference for the visuo-perceptual condition was set at a median of 6% at both time points. Regarding behavioural performance during the functional MRI experiment, there was no statistically significant interaction between condition and time on reaction time ($F = 0.142$, $P = 0.93$) nor on accuracy ($F = 0.226$, $P = 0.88$). The effect of time on reaction time was significant for all four conditions ($P_{corrected} < 0.0001$): reaction times were longer at time point 2 compared with time point 1 (Fig. 3A and Table 3). Time had no significant effect on accuracy for any of the conditions (Fig. 3B and Table 3).

Primary outcome analyses

As the primary outcome analysis, we performed a VOI-based voxel-wise regression analysis with change in amyloid load as predictor and, as outcome variable, the longitudinal change in BOLD response during the associative-semantic minus the visuo-perceptual condition. In the VOI, the increase in amyloid Centiloid score correlated positively with the difference in response amplitude during the associative-semantic versus the visuo-perceptual condition in the fundus and upper wall of the right STS ($x = 51$ mm, $y = -31$ mm, $z = 5$ mm, $Z = 3.53$, $P_{corrected} = 0.008$). Those individuals who showed more amyloid accumulation, showed a higher activity in this right posterior temporal activity focus at the second versus the first time point (Fig. 4B and C). No significant differences were observed in the remainder of the VOI (including the left posterior temporal cortex). The right STS focus of differential activation did not show a difference in BOLD response change between subjects scanned on the Intera versus the Achieva system at baseline ($P = 0.702$).

We evaluated how the longitudinal changes in functional MRI response related to changes in offline measures on the two computerized language tasks testing confrontation naming and lexical decision. The increase in functional MRI BOLD response during the associative-semantic versus the visuo-perceptual task in the right STS correlated significantly with a decrease in accuracy for the offline confrontation naming task. Higher activity in the right STS at the second versus the first time point correlated with lower confrontation naming accuracy scores (Pearson $R = -0.5$, $P_{corrected} = 0.016$) (Fig. 4D). No significant correlation was found with reaction times on the confrontation naming task nor with the lexical decision performance parameters. Increases in amyloid load did not correlate with change in offline experimental language test scores.

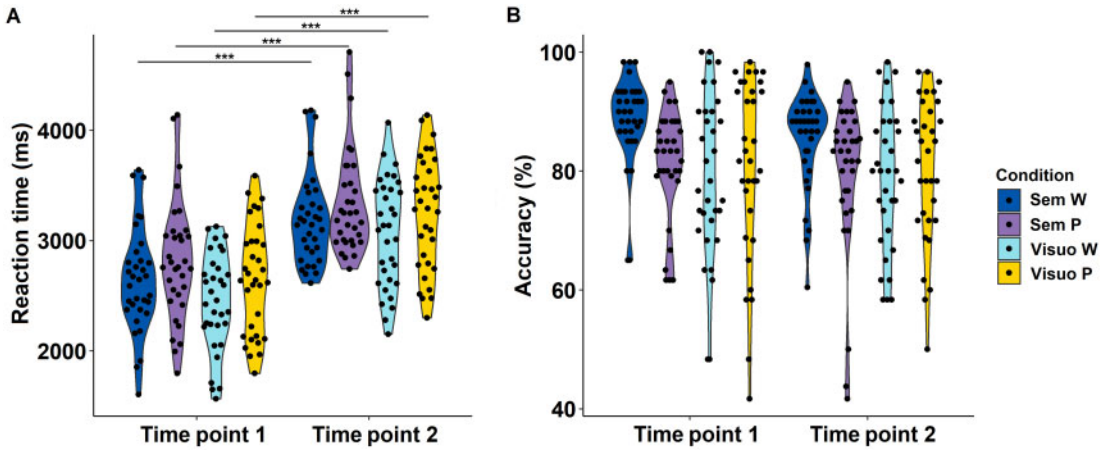

Figure 3 Behavioural scores on the Pyramids and Palm Trees Task. (**A**) Violin plot of reaction time per condition per time point (time point 1 versus time point 2). Significance is indicated as ***P < 0.001. (**B**) Violin plot of accuracy per condition per time point. Sem P/W = associative-semantic task with pictures/words; Visuo P/W = visuo-perceptual task with pictures/words.

To dissect the effect of amyloid accumulation on the change in activity during the associative-semantic versus visuo-perceptual condition in further detail, the VOI-based voxel-wise regression analysis was repeated for the associative-semantic minus visuo-perceptual condition for words and pictures separately. The difference in response amplitude in the right STS during the associative-semantic versus the visuo-perceptual condition for pictures at the second versus the first time point correlated positively with the difference in amyloid load in the composite VOI (x = 51 mm, y = –31 mm, z = 5 mm; Z = 3.88, $P_{corrected}$ = 0.002). No significant effect was obtained for words. When we lowered the threshold to an uncorrected *P*-value of 0.05, a correlation was also found for the word condition between change in amyloid load in the composite VOI and the difference in response amplitude in the right STS (x = 45 mm, y = –37 mm, z = –1 mm; Z = 1.94, voxel-level $P_{uncorrected}$ = 0.026, $P_{corrected}$ = 0.978).

In the whole-brain analysis, reduced activity in the left inferior frontal sulcus (IFS) region (x = –30 mm, y = 23 mm, z = 26 mm, extent = 61 voxels, cluster level $P_{corrected}$ = 0.009) (Fig. 5A and B) as well as in the right dorsomedial prefrontal cortex (x = 3 mm, y = 23 mm, z = 56 mm, extent = 69 voxels, cluster level $P_{corrected}$ = 0.005) correlated with increased amyloid (Fig. 5A and C). This indicates a decrease in functional response as brain amyloidosis increases. There was no statistically significant difference in the functional MRI BOLD response change in the left IFS (*P* = 0.70) and the right dorsomedial prefrontal focus (*P* = 0.89) between subjects scanned on the Intera versus the Achieva system at baseline.

For these two activity foci, no significant correlation was found between the mean functional MRI BOLD response change of the activity focus and performance on the experimental language tests after correction for multiple comparisons. In addition, no significant correlations between functional MRI BOLD response change and changes in reaction time, nor with accuracy during the Pyramids and Palm trees functional MRI task were observed.

The whole-brain analysis was repeated for the associative-semantic minus visuo-perceptual condition for words and pictures separately. Reduced activity in the left IFS during the associative-semantic versus the visuo-perceptual condition for pictures at the second versus the first time point correlated with increased amyloid load (x = –30 mm, y = 26 mm, z = 26 mm, extent = 46 voxels, cluster level $P_{corrected}$ = 0.035). When we lowered the threshold to an uncorrected *P*-value of 0.001, a correlation was also found for the word condition between change in amyloid load in the composite VOI and the difference in response amplitude in the left IFS (x = –36 mm, y = 23 mm, z = 23 mm; Z = 3.43, voxel-level $P_{uncorrected}$ < 0.001, $P_{corrected}$ = 0.698) and in the right dorsomedial prefrontal cortex (x = 3 mm, y = 23 mm, z = 56 mm; Z = 4.41, voxel-level $P_{uncorrected}$ < 0.001, $P_{corrected}$ = 0.046).

Secondary outcome analyses

Both a region-based and a whole-brain voxel-wise regression analysis were performed with a cross-sectional measure of tau load at time point 2 in the early metaVOI, as predictor, and as outcome variable the longitudinal change in functional MRI BOLD response during the associative-semantic minus the visuo-perceptual condition. No significant effects were obtained.

A linear regression analysis between grey matter volume change in the posterior temporal VOI and change in functional MRI activity levels did not yield a significant effect ($P_{corrected}$ > 0.2). Neither was there a significant effect in the whole-brain voxel-wise linear regression analysis with global grey matter change as regressor and change in functional MRI activity levels at the whole-brain level (voxel-level $P_{uncorrected}$ > 0.001).

In the VOI-based analysis, when grey matter volume change in the posterior temporal VOI was added as a covariate in the regression analysis between amyloid change and change in functional MRI activity levels, the results remained essentially the same (right posterior STS: x = 51 mm, y = –31 mm, z = 5 mm; Z = 3.61, $P_{corrected}$ = 0.006).

In the whole-brain voxel-wise regression analysis, when global grey matter volume was added as a covariate, the result in the right dorsomedial prefrontal cortex remained essentially the same (x = 3 mm, y = 23 mm, z = 56 mm, extent = 51 voxels, cluster level $P_{corrected}$ = 0.017), while the result in the left IFS region dropped just below the significance threshold (x = –30 mm, y = 23 mm, z = 26 mm, extent = 34 voxels, cluster level $P_{corrected}$ = 0.056).

Discussion

Longitudinal within-subject studies of change in cognitive brain circuits in the asymptomatic stage of Alzheimer's disease over a long time course are rare. Such studies are critical to understanding the resilience of cognitive brain circuits during the preclinical phase of the disease, an important theme given the long and protracted course of this preclinical phase and its increasing

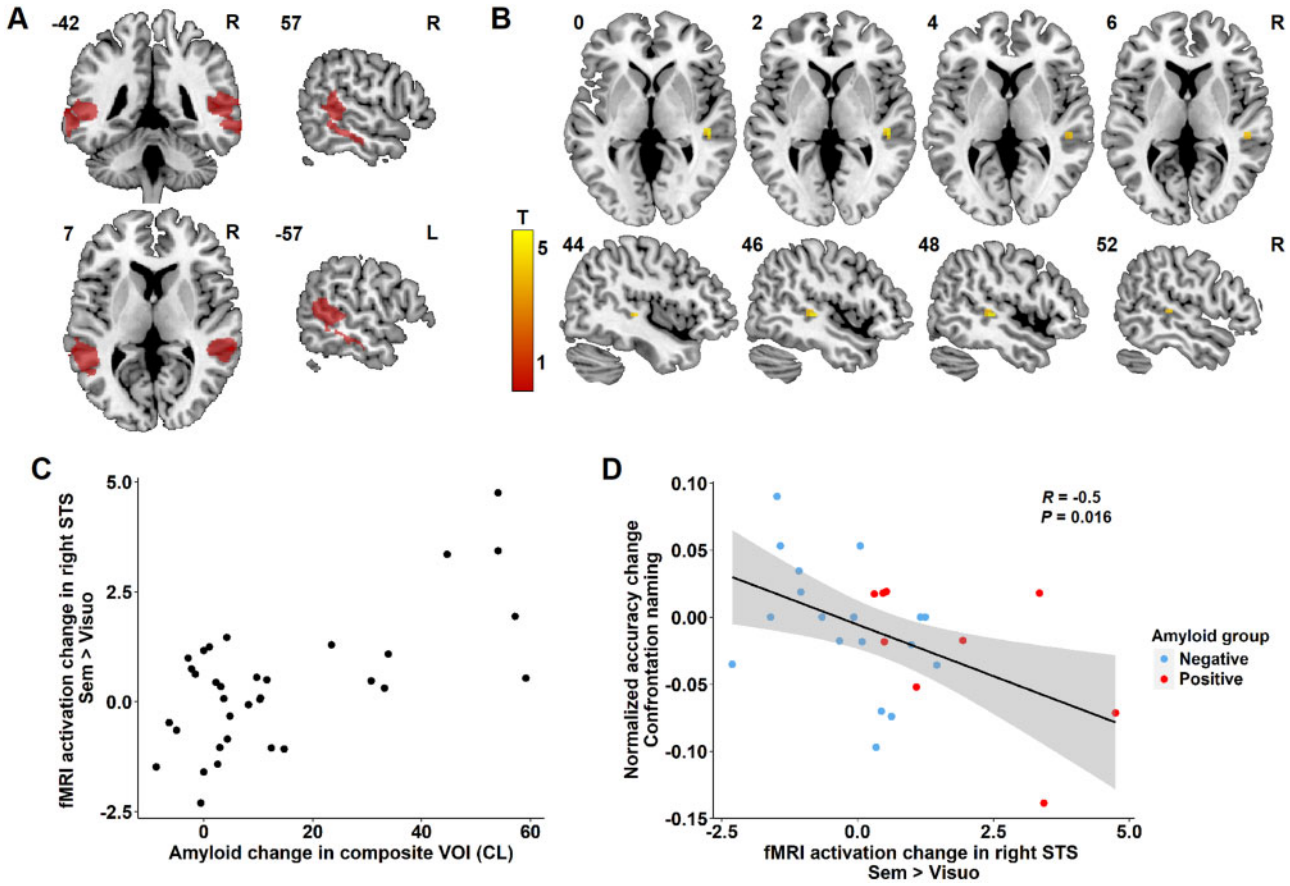

Figure 4 Region-based regression analysis. (**A**) Region of interest comprising the bilateral STS for the analysis, indicated in red. (**B**) Region of significant correlation between amyloid change in the composite VOI and functional MRI activation change during the associative-semantic minus visuo-perceptual condition in the right posterior STS (peak 51, –31, 5, voxel-level $P_{corrected}$ = 0.008). The colour scale indicates the *T*-values. MNI coordinates are indicated in the *top left* corner and orientation of the brain in the *top right* corner (R = right). (**C**) Relation between amyloid accumulation in the composite VOI expressed in Centiloids (CL) and functional MRI activation change during the associative-semantic minus the visuo-perceptual condition for time point 2 versus time point 1 in the right STS for illustrative purpose. (**D**) Correlation between change in functional MRI activation in the right STS VOI during the associative-semantic minus visuo-perceptual condition and the normalized change in confrontation naming accuracy scores for time point 2 versus time point 1 (Pearson *R* = –0.5, $P_{corrected}$ = 0.016). Amyloid-negative and amyloid-positive cases at follow-up are indicated in blue and red, respectively.

relevance for early intervention. Here we examined whether changes in amyloid load are associated with functional changes in the language circuit over an average period of 6 years in cognitively intact older adults, with a special focus on left and right posterior temporal cortex.[14,15,17] We also examined whether any such effect was mediated via aggregated tau given the narrow connection between the spread of tangles beyond medial temporal cortex and cognitive symptomatology. The primary hypothesis was confirmed: as amyloid accumulates in cognitively intact older adults, right posterior temporal cortex increased in activity (Fig. 4B and C). The increase in right posterior temporal activity correlated with a decrease in offline confrontation naming performance (Fig. 4D). These changes could not be accounted for by increased tau aggregation levels. Furthermore, in an exploratory whole-brain analysis, amyloid accumulation was associated with a decrease of activity in the left IFS and the dorsomedial prefrontal cortex, regions typically implicated in semantic and cognitive control, respectively.

The posterior third of the left STS is a key node in the language network, close to or overlapping with what has been classically called 'Wernicke's area' in the neurological jargon,[48] although debate exists about its exact anatomical boundaries and the contemporary usefulness of this eponym deeply engrained in neurological history.[49] Damage of this region due to stroke in the territory of the inferior branch of the middle cerebral artery is associated with word comprehension deficits.[48,50] The posterior STS has a word-specific role and has been implicated in lexical-semantic retrieval, while the posterior MTG is amodal and involved in semantic processing of both words and pictures.[51–54] The cortex in the fundus and the upper and lower wall of the left and right STS has been consistently implicated in word intelligibility by a large series of imaging studies.[15,28,52–54]

Previous task-related functional MRI studies on various stages of Alzheimer's disease have highlighted response amplitude changes in posterior temporal cortex. For instance, in cognitively intact APOE ε4 carriers with a family history of Alzheimer's disease who perform a famous name discrimination with famous versus unfamiliar names, activity in the right posterior temporal cortex is higher than in controls who do not have this Alzheimer's disease risk factor.[16] The right-sided posterior temporal increase was also present in amnestic mild cognitive impairment patients under the same task conditions.[16]

In the current study, while the posterior temporal location is in agreement with the *a priori* hypothesis, the direction of the activity change in left and right posterior temporal cortex did not exactly match the predictions based on prior studies.[14,17] To start, in the left posterior temporal cortex, a cross-sectional study in

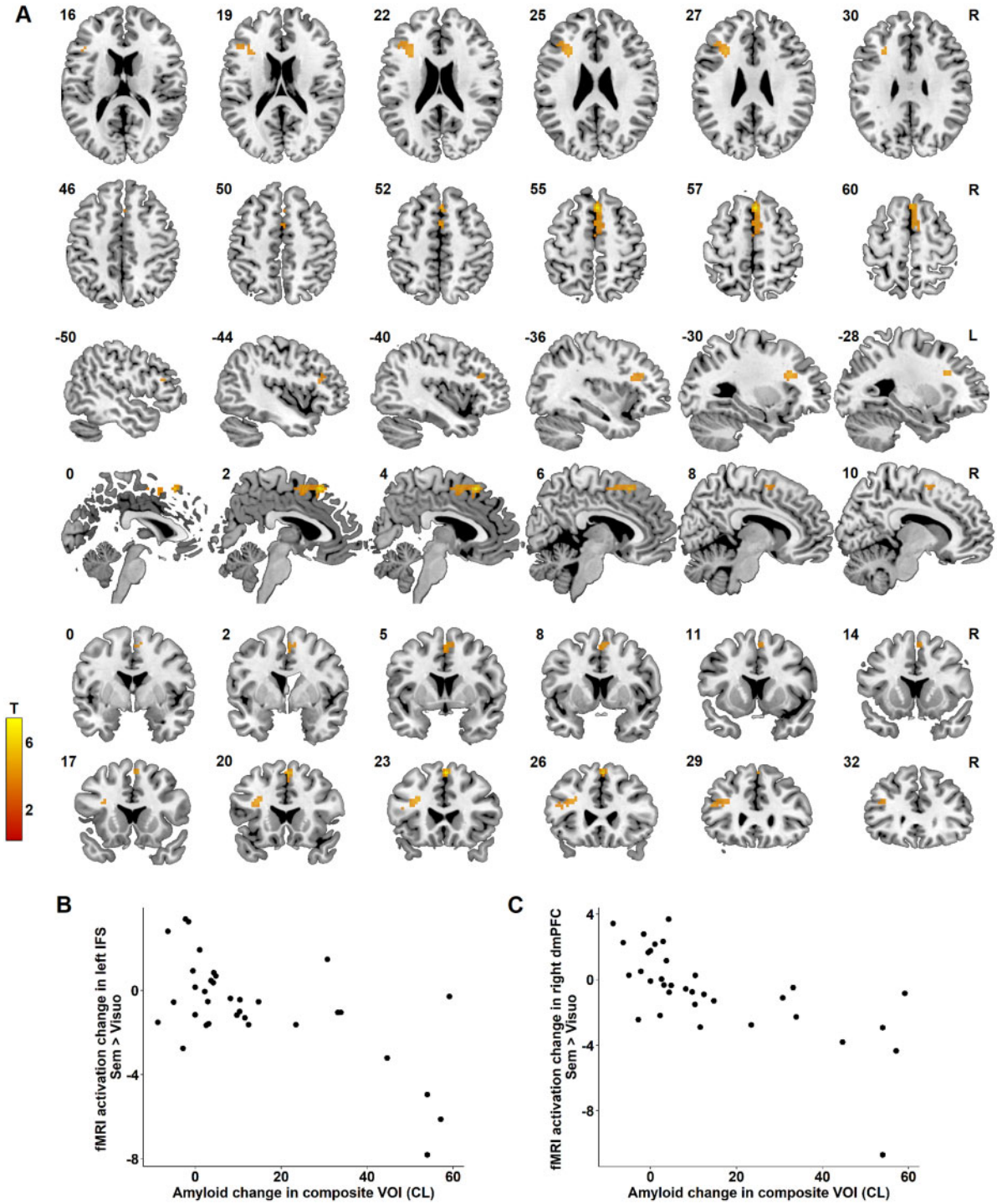

Figure 5 Whole-brain regression analysis. (**A**) Region of significant correlation between amyloid change in the composite VOI and functional MRI activation change during the associative-semantic minus visuo-perceptual condition in the left IFS (cluster peak –30, 23, 26, cluster-level $P_{corrected}$ = 0.009) and the right dorsomedial prefrontal cortex (cluster peak 3, 23, 56, cluster level $P_{corrected}$ = 0.005). The colour scale indicates the *T*-values. MNI coordinates are indicated in the *top left* corner and orientation of the brain in the *top right* corner. (**B** and **C**) Relation between amyloid accumulation in Centiloids (CL) and the change in functional MRI activation during the associative-semantic minus the visuo-perceptual condition in (**B**) the left IFS and (**C**) the right dorsomedial prefrontal cortex (dmPFC).

cognitively intact older adults found an increase in activity with higher amyloid load.[14] The same study reported a weak positive correlation between amyloid load and confrontation naming reaction times.[14] From this, one could have expected a longitudinal increase in response of left posterior temporal cortex with increasing amyloid, which was not observed. Conversely, the increase in right posterior temporal cortex confirmed the predictions based on Nelissen *et al.*,[17] both in terms of location and direction of change.

It is widely accepted that the right temporal neocortex contralateral to the left language network can contribute to word comprehension.[55–57] The right posterior MTG and STS has been

previously reported to show functional MRI response changes in language recovery following stroke[58] (for a review see Schevenels *et al.*[59]). An increase in the right STS and MTG has also been reported in amyloid PET-positive Alzheimer's disease in the early dementia stage.[17] In post-stroke aphasia the functional activity increases seen in homologous right-hemispheric language regions are generally considered less beneficial for recovery than increases in the surroundings of the lesioned left-sided region.[60] In the current study the increase in response amplitude correlated with an increased proportion of naming errors on an offline confrontation naming task. Under the hypothesis of a compensatory response, this would already imply that the compensation is insufficient. Theoretically, the right-hemispheric posterior temporal hyperactivation could also be harmful. Non-invasive inhibitory brain stimulation of right inferior frontal gyrus or right STS has not allowed the resolution of this issue unequivocally yet.[59,61] Based on the published studies, overall there seems to be a potential beneficial effect of inhibitory non-invasive stimulation of these regions in post-stroke aphasia but publication bias and small effect sizes render interpretation difficult.

In cognitively intact older adults, when amyloid load is high, the response in the right IFS with higher executive demands is reduced.[12] The findings in our longitudinal study are in line with this observation: the associative-semantic task is demanding and requires more executive control than the visuo-perceptual control task. As amyloid accumulates, the IFS response to higher cognitive control demands becomes attenuated. In our study, the effect occurred to the left with also a subthreshold effect in the right IFS. The left-sided predominance may well relate to the verbal and semantic nature of our task while the task in Oh *et al.*[12] was based on colours, isolated vowels and consonants. The left-sided IFS has been implicated in semantic control in numerous previous studies (for reviews see Noonan *et al.*[62] and Jackson[63]). These experiments are typically based on tasks similar to the associative-semantic task used in the current experiment. They manipulate semantic control by varying the association strength between sample and test stimuli, among other ways.[63] The dorsomedial prefrontal cortex has also been found bilaterally relatively consistently in these studies.[62,63] It is part of the multi-demand network,[64] a domain-general cognitive control system, and consists of Glasser *et al.*[65] areas 8BM and SCEF. The correspondence between these previous foci and the current results lends further credibility to the outcome of the whole-brain voxel-wise analysis results. The findings demonstrate the subclinical alterations in the cognitive control network in preclinical Alzheimer's disease. These findings in the semantic domain are highly complementary to similar prefrontal effects on cognitive control found previously in the non-verbal domain.[12]

It is well accepted that the amount of tau aggregates relates better to cognitive scores and Alzheimer's disease clinical severity stage than amyloid-β.[66] We hypothesized that in the asymptomatic stage, tau aggregation would be more closely related to functional brain activity changes than amyloid load but this was not the case. In cognitively normal older adults, the proportion of cases with increased tau in early vulnerable regions is generally relatively low, as is also the case in the current study (Fig. 2C). Tau PET has low sensitivity for the earliest Braak stages, i.e. Braak 1–3.[67,68] Early changes in phosphorylation of tau and fibril formation precede tau aggregation[69] and that would also not be detected by current tau PET radio-ligands.

The current findings highlight the importance of amyloid as a marker of asymptomatic Alzheimer's disease and establishes an association with the organization of cognitive brain circuits. The data suggest a link between amyloid accumulation and functional brain organization at a neuroanatomical scale, which is not mediated via grey matter volume change or tau aggregation. However, the relation between amyloid accumulation and functional changes in cognitive brain circuitry could still be indirect. For instance, the amyloid load could serve as a proxy or a 'timer' of where the individual is in the Alzheimer's disease pathophysiological process. Amyloid accumulation indicates the rising phase of amyloid-β aggregation. During this phase, specific pathophysiological processes may be active, the mechanism of which may be non-amyloidogenic. In that case, amyloid accumulation is a temporal marker of the disease stage rather than a direct cause.

Study limitations

Theoretically, amyloid in the blood vessel wall may affect the haemodynamic response, which is the basis of the BOLD signal. However, this would not explain the regional specificity nor the observation that some regions show a positive and others a negative effect of accumulating amyloid on the functional response.

Two different amyloid PET tracers were used; however, a consistent shift in values between tracers will not have an effect on the regression coefficient with functional MRI response amplitude change. This issue is further resolved by the use of Centiloid scale.[41] The MRI scanner used was not identical at the two time points in a subset of cases. This was systematically included as a covariate in all analyses, and furthermore, no effect was observed of the difference in MRI scanner.

Conclusion

This 6-year longitudinal multimodal imaging study provides insight into functional changes occurring during the rising phase of amyloid accumulation. It confirms the vulnerability of the posterior temporal nodes of the language network to Alzheimer's disease in this early, asymptomatic stage. It also demonstrates that amyloid accumulation is associated with functional effects on prefrontal cognitive control regions at this early stage.

Acknowledgements

We would like to thank the staff of Nuclear Medicine, Neurology, and Radiology at the University Hospitals Leuven. Special thanks to Carine Schildermans, Dorien Timmers, Kwinten Porters, Jef Van Loock, Mieke Steukers, Charlotte Evenepoel, Veerle Neyens, Tarik Jamoulle and Kelly Hilven for help with the study.

Funding

This work was supported by the Foundation for Alzheimer Research SAO-FRMA (09013, 11020, 13007); Research Foundation Flanders (G.0660.09, G094418N); KU Leuven (OT/08/056, OT/12/097, C14/17/108); IWT Vlaamse Impulsfinanciering voor Netwerken voor Dementie-onderzoek; Research Foundation Flanders senior clinical investigator grant to R.V. and K.V.L.; ^{18}F-flutemetamol was provided by GE Healthcare free of charge for this academic investigator-driven trial. The AV1451 precursor was provided free of charge via a material transfer agreement between R.V.'s institution and Avid Radiopharmaceuticals, a wholly-owned subsidiary to EliLilly (AV1451-EXIST-19). J.S. is a junior postdoctoral fellow of the FWO (12Y1620N).

Competing interests

None of the authors report disclosures relevant to the manuscript. R.V. has received research grants from Research Foundation—

Flanders (FWO) and KU Leuven. His institution has had a clinical trial agreement for phase 1 and 2 study with GEHC (R.V. as PI) and has received a non-financial support from GEHC (provision of ^{18}F-flutemetamol for conduct of investigator-driven trial free of cost) and from Avid Radiopharmaceuticals (provision of AV1451 precursor for this trial free of cost). R.V.'s institution has clinical trial agreements (with R.V. as local principal investigator) with Merck, Biogen, AbbVie, Roche, Johnson & Johnson and UCB. K.V.L. has received speaker fees from GEHC.

Supplementary material

Supplementary material is available at *Brain* online.

References

1. Forbes K, Venneri A, Shanks M. Distinct patterns of spontaneous speech deterioration: An early predictor of Alzheimer's disease. *Brain Cogn*. 2002;48(2-3):356–361.
2. Garrard P, Maloney L, Hodges J, Patterson K. The effects of very early Alzheimer's disease on the characteristics of writing by a renowned author. *Brain*. 2005;128(Pt 2):250–260.
3. Mueller K, Koscik R, Turkstra L, et al. Connected language in late middle-aged adults at risk for Alzheimer's disease. *J Alzheimers Dis*. 2016;54(4):1539–1550.
4. Dubois B, Feldman H, Jacova C, et al. Advancing research diagnostic criteria for Alzheimer's disease: The IWG-2 criteria. *Lancet Neurol*. 2014;13(6):614–629.
5. Sperling RA, Aisen PS, Beckett LA, et al. Toward defining the preclinical stages of Alzheimer's disease: Recommendations from the National Institute on Aging-Alzheimer's Association workgroups on diagnostic guidelines for Alzheimer's disease. *Alzheimers Dement*. 2011;7(3):280–292.
6. Bookheimer S, Strojwas M, Cohen M, et al. Patterns of brain activation in people at risk for Alzheimer's disease. *N Engl J Med*. 2000;343(7):450–456.
7. Bondi M, Houston W, Eyler L, Brown G. fMRI evidence of compensatory mechanisms in older adults at genetic risk for Alzheimer disease. *Neurology*. 2005;64(3):501–508.
8. Fleisher A, Houston W, Eyler L, et al. Identification of Alzheimer disease risk by functional magnetic resonance imaging. *Arch Neurol*. 2005;62(12):1881–1888.
9. Dickerson B. Functional magnetic resonance imaging of cholinergic modulation in mild cognitive impairment. *Curr Opin Psychiatry*. 2006;19(3):299–306.
10. Sperling R. Functional MRI studies of associative encoding in normal aging, mild cognitive impairment, and Alzheimer's disease. *Ann N Y Acad Sci*. 2007;1097:146–155.
11. Bakker A, Krauss G, Albert M, et al. Reduction of hippocampal hyperactivity improves cognition in amnestic mild cognitive impairment. *Neuron*. 2012;74(3):467–474.
12. Oh H, Steffener J, Razlighi Q, Habeck C, Stern Y. β-amyloid deposition is associated with decreased right prefrontal activation during task switching among cognitively normal elderly. *J Neurosci*. 2016;36(6):1962–1970.
13. König A, Satt A, Sorin A, et al. Automatic speech analysis for the assessment of patients with predementia and Alzheimer's disease. Alzheimer's Dement (Amst). 2015;1(1):112–124.
14. Adamczuk K, De Weer A-S, Nelissen N, et al. Functional changes in the language network in response to increased amyloid β deposition in cognitively intact older adults. *Cereb Cortex*. 2017;27(7):3879.
15. Vandenbulcke M, Peeters R, Dupont P, Van Hecke P, Vandenberghe R. Word reading and posterior temporal dysfunction in amnestic mild cognitive impairment. *Cereb Cortex*. 2007;17(3):542–551.
16. Woodard J, Seidenberg M, Nielson K, et al. Semantic memory activation in amnestic mild cognitive impairment. *Brain*. 2009;132(Pt 8):2068–2078.
17. Nelissen N, Vandenbulcke M, Fannes K, et al. Abeta amyloid deposition in the language system and how the brain responds. *Brain*. 2007;130(Pt 8):2055–2069.
18. Montembeault M, Chapleau M, Jarret J, et al. Differential language network functional connectivity alterations in Alzheimer's disease and the semantic variant of primary progressive aphasia. *Cortex*. 2019;117:284–298.
19. Arriagada PV, Growdon JH, Hedley-Whyte ET, Hyman BT. Neurofibrillary tangles but not senile plaques parallel duration and severity of Alzheimer's disease. *Neurology*. 1992;42(3 Pt 1):631–639.
20. Okamura N, Harada R, Furumoto S, Arai H, Yanai K, Kudo Y. Tau PET imaging in Alzheimer's disease. *Curr Neurol Neurosci Rep*. 2014;14(11):500.
21. Schaeverbeke J, Gabel S, Meersmans K, et al. Baseline cognition is the best predictor of 4-year cognitive change in cognitively intact older adults. *Alzheimer's Res Ther*. 2021;13(1):75.
22. Mariën P, Mampaey E, Vervaet A, Saerens J, De Deyn P. Normative data for the Boston naming test in native Dutch-speaking Belgian elderly. *Brain Lang*. 1998;65(3):447–467.
23. Bastiaanse R, Bosje M, Visch-Brink E. *Psycholinguïstische testbatterij voor de taalverwerking van afasiepatiënten (PALPA)*. Lawrence Erlbaum Associates; 1995.
24. Laiacona M, Capitani E. A case of prevailing deficit of nonliving categories or a case of prevailing sparing of living categories? *Cogn Neuropsychol*. 2001;18(1):39–70.
25. Snodgrass J, Vanderwart M. A standardized set of 260 pictures: Norms for name agreement, image agreement, familiarity, and visual complexity. *J Exp Psychol Hum Learn*. 1980;6(2):174–215.
26. Snodgrass J, Levy-Berger G, Haydon M. Human experimental psychology. Oxford University Press; 1985. Accessed 30 September 2021. https://psycnet.apa.org/record/1985-98269-000
27. Pallier C. Computing discriminability and bias with the R software; 2002. Accessed 30 September 2021. https://www.pallier.org/pdfs/aprime.pdf
28. Vandenberghe R, Price C, Wise R, Josephs O, Frackowiak R. Functional anatomy of a common semantic system for words and pictures. *Nature*. 1996;383(6597):254–256.
29. Vandenbulcke M, Peeters R, Van Hecke P, Vandenberghe R. Anterior temporal laterality in primary progressive aphasia shifts to the right. *Ann Neurol*. 2005;58(3):362–370.
30. Vandenbulcke M, Peeters R, Fannes K, Vandenberghe R. Knowledge of visual attributes in the right hemisphere. *Nat Neurosci*. 2006;9(7):964–970.
31. Nelissen N, Dupont P, Vandenbulcke M, Tousseyn T, Peeters R, Vandenberghe R. Right hemisphere recruitment during language processing in frontotemporal lobar degeneration and Alzheimer's disease. *J Mol Neurosci*. 2011;45(3):637–647.
32. Vandenberghe R, Wang Y, Nelissen N, et al. The associative-semantic network for words and pictures: Effective connectivity and graph analysis. *Brain Lang*. 2013;127(2):264–272.
33. Howard D, Patterson K. *Pyramids and Palm Trees: A test of semantic access from pictures and words*. Thames Valley Test Co.; 1992.
34. Chételat G, Landeau B, Eustache F, et al. Using voxel-based morphometry to map the structural changes associated with rapid conversion in MCI: A longitudinal MRI study. *Neuroimage*. 2005;27(4):934–946.

35. Koole M, Lewis D, Buckley C, et al. Whole-body biodistribution and radiation dosimetry of 18F-GE067: A radioligand for in vivo brain amyloid imaging. *J Nucl Med*. 2009;50(5):818–822.
36. Nelissen N, Van Laere K, Thurfjell L, et al. Phase 1 study of the Pittsburgh compound B derivative 18F-flutemetamol in healthy volunteers and patients with probable Alzheimer disease. *J Nucl Med*. 2009;50(8):1251–1259.
37. Vandenberghe R, Van Laere K, Ivanoiu A, et al. 18F-flutemetamol amyloid imaging in Alzheimer disease and mild cognitive impairment: A phase 2 trial. *Ann Neurol*. 2010;68(3):319–329.
38. Vandenberghe R, Nelissen N, Salmon E, et al. Binary classification of ^{18}F-flutemetamol PET using machine learning: Comparison with visual reads and structural MRI. *Neuroimage*. 2013;64:517–525.
39. De Meyer S, Schaeverbeke JM, Verberk IMW, et al. Comparison of ELISA- and SIMOA-based quantification of plasma Aβ ratios for early detection of cerebral amyloidosis. *Alzheimers Res Ther*. 2020;12(1):162.
40. Schwarz C, Gunter J, Lowe V, et al. A comparison of partial volume correction techniques for measuring change in serial amyloid PET SUVR. *J Alzheimer's Dis*. 2019;67(1):181–195.
41. Klunk W, Koeppe R, Price J, et al. The Centiloid Project: Standardizing quantitative amyloid plaque estimation by PET. *Alzheimers Dement*. 2015;11(1):1–4.
42. Adamczuk K, Schaeverbeke J, Nelissen N, et al. Amyloid imaging in cognitively normal older adults: Comparison between (18)F-flutemetamol and (11)C-Pittsburgh compound B. *Eur J Nucl Med Mol Imaging*. 2016;43(1):142–151.
43. La Joie R, Ayakta N, Seeley WW, et al. Multisite study of the relationships between antemortem [(11)C]PIB-PET Centiloid values and postmortem measures of Alzheimer's disease neuropathology. *Alzheimers Dement*. 2019;15(2):205–216.
44. Amadoru S, Doré V, McLean CA, et al. Comparison of amyloid PET measured in Centiloid units with neuropathological findings in Alzheimer's disease. *Alzheimers Res Ther*. 2020;12(1):22.
45. Rosseel Y. Lavaan: An R package for structural equation modeling and more. Version 0.5–12 (BETA). *J Stat Softw*. 2012;48(2):1–36.
46. Singmann H, Bolker B, Westfall J, Aust F. afex: Analysis of Factorial Experiments. R package; 2018.
47. Fan L, Li H, Zhuo J, et al. The human Brainnetome atlas: A new brain atlas based on connectional architecture. *Cereb Cortex*. 2016;26(8):3508–3526.
48. Hillis A, Wityk R, Tuffiash E, et al. Hypoperfusion of Wernicke's area predicts severity of semantic deficit in acute stroke. *Ann Neurol*. 2001;50(5):561–566.
49. Binder JR. The Wernicke area: Modern evidence and a reinterpretation. *Neurology*. 2015;85(24):2170–2175.
50. Bonilha L, Hillis A, Hickok G, den Ouden D, Rorden C, Fridriksson J. Temporal lobe networks supporting the comprehension of spoken words. *Brain*. 2017;140(9):2370–2380.
51. Scott SK, Blank CC, Rosen S, Wise RJ. Identification of a pathway for intelligible speech in the left temporal lobe. *Brain*. 2000;123 (Pt 12):2400–2406.
52. Davis MH, Johnsrude IS. Hierarchical processing in spoken language comprehension. *J Neurosci*. 2003;23(8):3423–3431.
53. Evans S, Kyong JS, Rosen S, et al. The pathways for intelligible speech: Multivariate and univariate perspectives. *Cereb Cortex*. 2014;24(9):2350–2361.
54. Obleser J, Kotz SA. Expectancy constraints in degraded speech modulate the language comprehension network. *Cereb Cortex*. 2010;20(3):633–640.
55. Kinsbourne M. The minor cerebral hemisphere as a source of aphasic speech. *Arch Neurol*. 1971;25(4):302–306.
56. Zaidel E. Auditory vocabulary of the right hemisphere following brain bisection or hemidecortication. *Cortex*. 1976;12(3):191–211.
57. Gainotti G. The riddle of the right hemisphere's contribution to the recovery of language. *Eur J Disord Commun*. 1993;28(3): 227–246.
58. Heiss WD, Kessler J, Thiel A, Ghaemi M, Karbe H. Differential capacity of left and right hemispheric areas for compensation of poststroke aphasia. *Ann Neurol*. 1999;45(4):430–438.
59. Schevenels K, Price CJ, Zink I, De Smedt B, Vandermosten M. A review on treatment-related brain changes in aphasia. *Neurobiol Lang*. 2020;1(4):402–433.
60. Heiss W-D. Contribution of neuro-imaging for prediction of functional recovery after ischemic stroke. *Cerebrovasc Dis*. 2017; 44(5-6):266–276.
61. Breining BL, Sebastian R. Neuromodulation in post-stroke aphasia treatment. *Curr Phys Med Rehabil Reports*. 2020;8(2): 44–56.
62. Noonan KA, Jefferies E, Visser M, Lambon Ralph MA. Going beyond inferior prefrontal involvement in semantic control: Evidence for the additional contribution of dorsal angular gyrus and posterior middle temporal cortex. *J Cogn Neurosci*. 2013; 25(11):1824–1850.
63. Jackson RL. The neural correlates of semantic control revisited. *Neuroimage*. 2021;224:117444.
64. Assem M, Glasser MF, Van Essen DC, Duncan J. A domain-general cognitive core defined in multimodally parcellated human cortex. *Cereb Cortex*. 2020;30(8):4361–4380.
65. Glasser MF, Coalson TS, Robinson EC, et al. A multi-modal parcellation of human cerebral cortex. *Nature*. 2016;536(7615): 171–178.
66. Grober E, Dickson D, Sliwinski MJ, et al. Memory and mental status correlates of modified Braak staging. *Neurobiol Aging*. 1999; 20(6):573–579.
67. Wren MC, Lashley T, Årstad E, Sander K. Large inter- and intra-case variability of first generation tau PET ligand binding in neurodegenerative dementias. *Acta Neuropathol Commun*. 2018; 6(1):34.
68. Fleisher AS, Pontecorvo MJ, Devous MDS, et al.; A16 Study Investigators. Positron emission tomography imaging with [18F]flortaucipir and postmortem assessment of Alzheimer disease neuropathologic changes. *JAMA Neurol*. 2020;77(7):829–839.
69. Aragão Gomes L, Uytterhoeven V, Lopez-Sanmartin D, et al. Maturation of neuronal AD-tau pathology involves site-specific phosphorylation of cytoplasmic and synaptic tau preceding conformational change and fibril formation. *Acta Neuropathol*. 2021;141(2):173–192.